Biophysical Journal Volume 96 January 2009 45–55

Structural Rearrangements in Loop F of the GABA Receptor Signal Ligand Binding, Not Channel Activation

Alpa Khatri, Anna Sedelnikova, and David S. Weiss*

Department of Physiology, University of Texas Health Science Center at San Antonio, San Antonio, Texas

ABSTRACT Structure-function studies of the Cys loop family of ionotropic neurotransmitter receptors (GABA, nACh, 5-HT_3, and glycine receptors) have resulted in a six-loop (A–F) model of the agonist-binding site. Key amino acids have been identified in these loops that associate with, and stabilize, bound ligand. The next step is to identify the structural rearrangements that couple agonist binding to channel opening. Loop F has been proposed to move upon receptor activation, although it is not known whether this movement is along the conformational pathway for channel opening. We test this hypothesis in the GABA receptor using simultaneous electrophysiology and site-directed fluorescence spectroscopy. The latter method reveals structural rearrangements by reporting changes in hydrophobicity around an environmentally sensitive fluorophore attached to defined positions of loop F. Using a series of ligands that span the range from full activation to full antagonism, we show there is no correlation between the rearrangements in loop F and channel opening. Based on these data and agonist docking simulations into a structural model of the GABA binding site, we propose that loop F is not along the pathway for channel opening, but rather is a component of the structural machinery that locks ligand into the agonist-binding site.

INTRODUCTION

γ-Aminobutyric acid (GABA) is the main inhibitory neurotransmitter in the mammalian central nervous system (1). The binding of GABA to its pentameric receptor on the postsynaptic membrane leads to the opening of an integral chloride pore that typically hyperpolarizes the neuron (in adults), thereby reducing excitability. The GABA receptor is a target for a variety of substances that can modulate its activity, including benzodiazepines, barbiturates, neurosteroids, anesthetics, and alcohol (2). Several decades of research have revealed insights into the mechanisms and structures that underlie GABA receptor activation, modulation, regulation, and permeation (3).

Fig. 1 *A* shows a structural model of the pentameric ρ1 GABA receptor determined via homology modeling from the acetylcholine-binding protein (AChBP). The original report of the AChBP structure confirmed the presence of six loops (A–F; colored in Fig. 1 *A*) at each subunit interface that form the agonist-binding site (4). Loops A–C are contributed by one subunit, and loops D–F are contributed by the neighboring subunit. For the pentameric $GABA_A$ receptor comprised of the prototypical α, β, and γ subunits with a 2:2:1 stoichiometry (5,6), there are two agonist-binding sites. For the homomeric $GABA_C$ receptor comprised of the five ρ1 subunits studied here, there are five putative binding sites, although on average only three GABA molecules need to bind agonist to gate the pore (7). Crucial amino acids have been identified in these loops that interact with ligand (8–15), and conformational changes have been revealed in the binding site in response to agonist (16–19). It is certain that at least some of these structural rearrangements transduce the binding of agonist to the opening of the gate in the ion pore. This gate is located some distance away from the agonist-binding site, presumably near the middle of the second transmembrane domain (20,21). Loop F (shown in *green* in Fig. 1 *A*, with the amino acid sequence provided in Fig. 1 *B*), owing to its location at the bottom of the binding cleft (4), has been proposed to be a key transduction element linking ligand binding to channel opening (22–24).

To date, there are three main approaches for inferring conformational rearrangements underlying receptor activation. One technique employs the state dependence of accessibility (25). In this method, cysteine residues are introduced at defined locations and the accessibility to modification of the free sulfhydryl side chains on these cysteines are compared when the channels are in different kinetic states (open, closed, or desensitized) (9,17,26). One complicating factor of this somewhat indirect method is that the presence of ligand itself, via steric hindrance of the accessibility reagent, can impair modification. Thus, one is not necessarily looking at conformational changes per se, but rather the ability of the modifying reagent to reach its target cysteine. A second method is structural resolution in combination with molecular modeling. The structural information has been derived mainly from electron microscopy of the nACh receptor (21,27,28) and x-ray crystallography of the acetylcholine-binding protein (4), the extracellular domain of the nACh receptor (29), and the recently crystallized prokaryotic member of this cys-loop family (30). Issues to consider are that the structures are static snapshots of the receptors in typically unknown kinetic states (open versus closed) and the modeling is limited by our incomplete understanding of the complex set of forces that determine structural stability and conformational dynamics. The third approach is site-directed

Submitted April 8, 2008, and accepted for publication September 24, 2008.

*Correspondence: weissd@uthscsa.edu

Editor: Richard W. Aldrich.

0006-3495/09/01/0045/11 $2.00

doi: 10.1016/j.bpj.2008.09.011

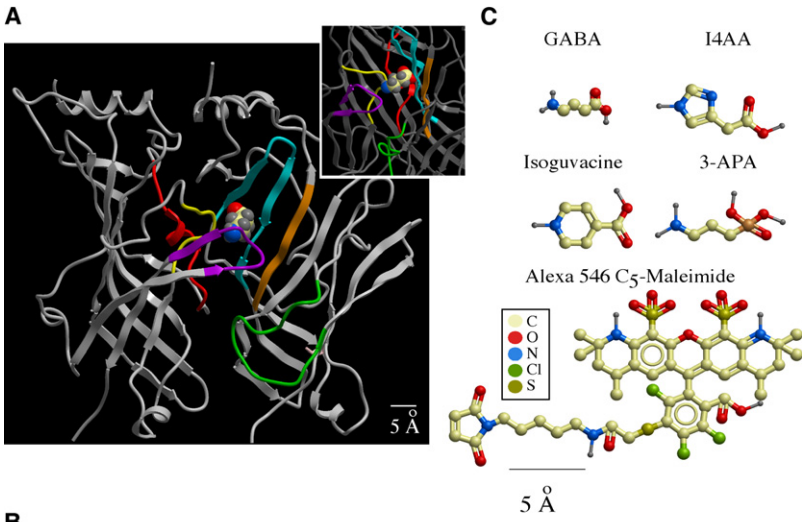

B

			216														231
human	GABAc	ρ1	**L**	**K**	**T**	D	E	R	I	**S**	L	S	Q	F	L	**I**	Q	E
rat	GABAA	α1	V	A	E	D	G	S	-	R	L	N	Q	Y	D	L	L	G
rat	GABAA	β2	V	T	G	V	T	K	I	E	L	P	Q	F	S	I	V	D
rat	GABAA	γ2	V	G	D	T	R	S	W	R	L	Y	Q	F	S	F	V	G
	AChBP		D	D	S	E	Y	F	S	Q	Y	S	R	F	E	I	L	D

FIGURE 1 Structures of the GABA receptor, ligands, and fluorophore. (*A*) Structural model of the human ρ1 $GABA_C$ extracellular domain constructed by homology with the AChBP. Two subunits comprising a single agonist-binding site are shown. The six loops that form the binding pocket are colored as follows: loop A, red; loop B, yellow; loop C, purple; loop D, brown; loop E, blue; loop F, green. The docked GABA molecule is shown in a preferred orientation with the amino group (*blue*) proximate to loop C, and the carboxylic acid group (oxygens in *red*) proximate to loop E. An expanded view of the GABA molecule in the binding site is also shown. (*B*) Aligned sequences of loop F for the $GABA_C$ receptor, three $GABA_A$ receptor subunits, and the AChBP. The five bold residues are the main amino acids investigated in this study. (*C*) Structures of the ligands utilized and Alexa 546 maleimide (A5m).

fluorescence spectroscopy, as employed here (16,18,31). In this method, an environmentally sensitive fluorophore is attached to cysteines introduced at defined positions in the receptor. Changes in hydrophobicity around the fluorophore produce measurable changes in fluorescence. Although this method identifies regional structural rearrangements, some caution must be used when interpreting these data. First, the fluorophores detect changes in environmental hydrophobicity, and not necessarily movement of the domain (cysteine) to which the fluorophore is attached. Another limitation is the size of the fluorophore and, although tethered, its rotational mobility. Still, this is a powerful new method that, when coupled with an electrophysiological analysis, can reveal insights into the dynamics of ion channel and receptor activation mechanisms (16,18,31,32).

In this study, using a combination of two-electrode voltage clamp and site-directed fluorescence spectroscopy, we tested the hypothesis that loop F in the agonist-binding site is a key element along the pathway coupling agonist binding to channel opening. Although we document structural rearrangements in this region, our data indicate that these rearrangements signal the presence of ligand, and not the degree of activation.

MATERIALS AND METHODS

cDNA and cRNA preparation

Site-directed mutagenesis was carried out with the use of standard polymerase chain reaction techniques described previously (10). The fragments were cloned into pGEMHE in the T7 orientation and the sequence was verified by automated DNA sequencing. cDNA was prepared for wild-type and mutant ρ1 subunits using a midi-prep kit (Promega, Madison, WI) and eluted with RNase free water (Ambion, Austin, TX). Ten micrograms of cDNA were linearized by Nhe I digestion (NEB Labs, Ipswich, MA) which was then used to prepare the cRNA. The Ambion T7 mMessage mMachine kit was used to transcribe the cDNA into capped cRNA that was eluted with nuclease free water (Ambion, Austin, TX).

Oocyte harvesting and cRNA injection

Female *Xenopus laevis* (*Xenopus* I, Dexter, MI) were anesthetized with 0.1% MS-222 (Sigma Aldrich, St. Louis, MO). Oocytes were surgically removed from the anesthetized frogs and washed with calcium-free OR2 (92.5 mM NaCl, 2.5 mM KCl, 10 mM HEPES, and 1 mM $MgCl_2$) at pH 7.5. This procedure was approved by the Institutional Animal Care and Use Committee of the University of Texas Health Science Center at San Antonio. The oocytes were defolliculated using 0.1–0.2% collagenase A (Roche Applied Science, Indianapolis, IN) in calcium-free OR2 for 1.5–2 h at room temperature. The oocytes were then washed and stored in ND96 (96 mM NaCl, 2 mM KCl, 1 mM $MgCl_2$, 5 mM HEPES, and 1.8 mM $CaCl_2$) with 5% horse serum (Invitrogen, Carlsbad, CA), 25 mM sodium pyruvate (Sigma Aldrich, St. Louis, MO) and 20 mg/L gentamicin (Invitrogen, Carlsbad, CA) at pH 7.5. Stage VI oocytes were sorted and stored at 16°C before injection of cRNA. Microinjection needles were prepared on a Sutter P-97 horizontal puller (Sutter Instrument, Novato, CA) and a Nanoject II microinjection system (Drummond Scientific, Broomall, PA) was used to inject the cRNA into the oocytes. The injected oocytes were incubated at 16°C for 3–4 days before labeling and recording.

Fluorophore labeling

Alexa Fluor 546 C_5 maleimide (A5m; Molecular Probes, Eugene, OR) was reconstituted with dimethyl sulfoxide to a 5 mM stock solution and stored at −20°C until needed. Oocytes were rinsed three times with OR2 before labeling. The A5m stock solution was diluted to 20 μM in OR2 at pH 7.2 before use. Oocytes were labeled for 30 min while they were slowly shaken at room temperature. After labeling, the oocytes were washed in OR2 (pH 7.5) twice and placed in the recording chamber. It should be mentioned that all five subunits carry the cysteine mutation, so there is a potential for pentameric labeling by A5m. Given that this is a presumably symmetric homomeric receptor, we assume that all five cysteines have an equal likelihood of being labeled. Although experiments demonstrated that our

labeling reaction reached saturation, we do not know the actual stoichiometry of the labeling.

Site-specific fluorescence spectroscopy

A two-electrode voltage clamp was used to measure the expression level of the injected oocytes. The labeled oocytes were placed in a unique recording chamber so that both fluorescence and current could be measured simultaneously (16). The chamber consists of two sections separated by a 0.8 mm aperture on which the oocyte sits. The oocyte was impaled for two-electrode voltage clamp in the top chamber, and agonist was applied in the lower chamber. An Axiovert 200 (Zeiss, Jena, Germany) was used to image the fluorescence from the bottom of the chamber. In this way, currents and fluorescence were recorded from the same subpopulation of receptors in the lower chamber.

The oocyte was clamped at −40 mV with a GeneClamp 500 (Axon Instruments, Foster City, CA) to measure the ligand-induced currents. A 90 W halogen bulb was used as the light source in the DeltaRAM monochromator (PTI, Birmingham, NJ). Light (546 nm) was passed into the microscope via a liquid light guide. The microscope holds dichroic (HQ570LP) and emission (HQ610/75m) filters (Chroma Technology, Brattleboro, VT) for fluorescence detection. The fluorescence signal was detected by a photomultiplier tube (R1527P Hamamatsu Photonics, Bridgewater, NJ) housed in the PTI model 814 and mounted on the side port of the microscope. The data were digitized at 20 Hz with an ITC-16 (InstruTECH, Port Washington, NY) connected to a Macintosh computer (Apple Computer, Cupertino, CA). The fluorescence and current data were recorded and analyzed by IGOR Pro (WaveMetrics, Lake Oswego, OR). The dose-dependent relation for the agonist was fitted with the following equation:

$$I = \frac{I_{max}}{1 + (EC_{50}/[A])^n} \quad (1)$$

where I is the current generated by a specific concentration of the agonist, $[A]$; I_{max} is the maximum current; EC_{50} is the concentration of $[A]$ that is required to obtain 50% of the I_{max}; and n is the Hill coefficient (slope). Student's t-test allowed us to compare the EC_{50} values for the mutants (L216C, K217C, T218, S223C, I229C, D219C, S225C, and L228C) before and after labeling with A5m, as well as ΔF and ΔI values between the different ligands. We used the following ligand concentrations: *trans*-aminocrotonic acid (TACA), 500 μM; GABA, 200 μM (for the I229C mutant we used 1000 μM); imidazole-4-acetic acid (I4AA), 1000 μM; isoguvacine, 1000 μM; and 3-aminopropylphosphonic acid (3-APA), 500 μM. In the case of agonists, these were saturating concentrations for channel activation (currents) determined from dose-response relations fit with Eq. 1. For the antagonist 3-APA, 500 μM gives complete block of receptor activation at lower agonist concentrations. The only exception was for L216C and I4AA, where 1000 μM was subsaturating and produced a current that was 68% of the maximum as determined from extrapolation of the dose-response relation. All agonists and antagonists were purchased from Sigma Aldrich.

Homology modeling and docking

A structural model was created for the amino terminal domain of the ρ1 subunit based on the AChBP crystal structure (PDB number 1i9b) (4) with the use of ICM Pro and Homology (Molsoft, San Diego, CA). The amino acid sequence was first aligned for the ρ1 subunit and the AChBP. Next, the amino terminal domain of the ρ1 subunit was threaded onto the AChBP crystal structure. Each subunit was modeled individually and regularized, correcting for the lack of hydrogens in the PDB structure. The modeled subunits also underwent a local energy minimization before being grouped as one object. After grouping, the side chains of the amino acids were energy-minimized and optimized to the lowest energy level to generate a model for ligand docking.

To set up the GABA docking project, we first identified potential ligand-binding sites. The interface for subunits A and E were chosen to dock GABA. A ligand probe was placed behind loop C and a box (24.0 × 26.4 × 24.3 Å) was placed around this potential ligand-binding area. Receptor maps were generated before GABA was docked into the rigid receptor model. GABA was docked into a rigid structure and generated 30 potential conformations. The orientation of GABA shown was the lowest energy of all the potential orientations.

RESULTS

Mutations and labeling have minor effects on channel activation

Residues in loop F of the ρ1 GABA receptor subunit were mutated to cysteine, one at a time, to provide a free sulfhydryl group to bind A5m. A previous cursory substituted cysteine accessibility method (SCAM) analysis of loop F demonstrated minor changes in receptor sensitivity with these cysteine mutations (10). Here, we extended this analysis to determine whether the attachment of A5m compromises receptor function. All available evidence indicates that the only available cysteine for fluorophore attachment is the cysteine introduced by mutagenesis (9,10). We also made the assumption that shifts in GABA sensitivity with incubation in A5m confirm that the cysteine residue is accessible and labeled by the fluorophore. Fig. 2 *A* shows representative currents from the K217C mutant before (*top traces*) and after (*bottom traces*) incubation in 20 μM A5m. The graph in Fig. 2 *B* is a plot of the dose-response relation (with and without A5m labeling) for the wild-type receptor and two representative mutants in loop F. The top section of Table 1 presents the EC_{50} values for the five loop F

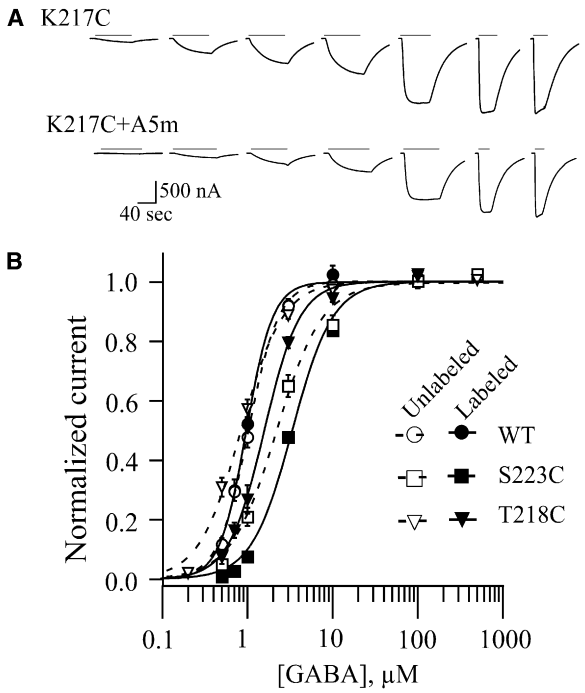

FIGURE 2 Dose-response relations of cysteine mutants before and after labeling with the fluorophore, A5m. (*A*) GABA-activated currents before (*top*) and after (*bottom*) labeling with A5m in the K217C mutant. (*B*) Dose-response relations for the wild-type receptor and two cysteine mutants before and after A5m labeling.

TABLE 1 Comparison of the dose-response relations for select mutants before and after A5m labeling

	Unlabeled			A5m Labeled		
Receptor	EC_{50} (μM)	Hill coefficient	n	EC_{50}(μM)	Hill coefficient	n
WT	0.98 ± 0.04	2.78 ± 0.21	3	1.04 ± 0.04	3.50 ± 1.00	3
L216C*	0.58 ± 0.05	1.50 ± 0.14	4	4.26 ± 0.11	3.87 ± 0.27	4
K217C*	1.09 ± 0.05	1.72 ± 0.27	3	1.48 ± 0.11	2.14 ± 0.15	5
T218C*	1.60 ± 0.11	2.10 ± 0.17	3	0.85 ± 0.06	1.80 ± 0.06	5
S223C*	3.39 ± 0.05	1.82 ± 0.03	3	2.34 ± 0.31	1.62 ± 0.08	5
I229C*	3.99 ± 0.43	1.97 ± 0.04	3	2.97 ± 0.07	2.04 ± 0.07	4
D219C*	3.49 ± 0.25	1.24 ± 0.01	3	5.02 ± 0.38	1.38 ± 0.01	3
S225C	0.41 ± 0.02	2.13 ± 0.10	3	0.46 ± 0.02	2.13 ± 0.03	3
L228C*	0.18 ± 0.02	2.37 ± 0.60	3	0.41 ± 0.004	1.97 ± 0.5	3

*Statistically significant difference between unlabeled and A5m labeled ($p < 0.05$).

residues that are central to this study (L216C, K217C, T218C, S223C, and I229C) plus three others to be discussed subsequently. Although there was a slight shift in GABA sensitivity with mutagenesis and labeling, the effect was surprisingly modest given the cysteine substitution and the attached fluorophore. Nevertheless, these data confirm what a previous SCAM analysis of loop F suggested in the $GABA_C$ (10) and $GABA_A$ receptors (22). Although the majority of loop F is accessible to modification, the impact of the cysteine substitutions and sulfhydryl modifications on agonist-mediated activation are modest, and this observation is relevant for a consideration of the role of loop F in the activation process.

Most residues in loop F demonstrate a GABA-mediated change in fluorescence

Oocytes expressing the mutant GABA receptors were labeled with A5m as described in Materials and Methods and then placed in the recording chamber for the simultaneous measurement of GABA-mediated changes in current (ΔI) and fluorescence (ΔF). This fluorophore can detect changes in the hydrophobicity of the surrounding environment via changes in its fluorescence intensity. Fig. 3 shows the putative structure of loop F (for orientation, see Fig. 1 *A*) with representative fluorescence changes in response to a saturating concentration of GABA. Although background fluorescence was detected in labeled oocytes expressing either wild-type GABA receptors or no GABA receptors at all, this would be expected since free and accessible sulfhydryl groups must certainly exist on endogenous oocyte membrane proteins and would therefore be labeled by the A5m. No change of fluorescence in response to GABA application was observed for oocytes expressing either wild-type receptors or no GABA receptors at all (noninjected oocytes).

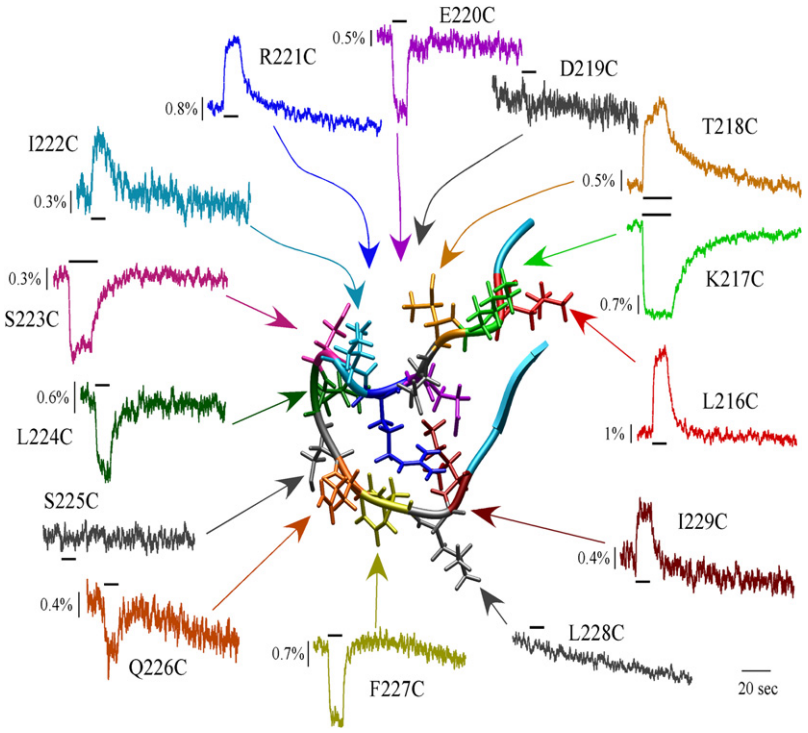

FIGURE 3 Fluorescence changes in loop F. Each residue in loop F was mutated to cysteine, one at a time, labeled with A5m, and then exposed to a saturating concentration of GABA. The positions that do not show a change in fluorescence in response to GABA are shown in gray.

Note that the direction of the fluorescence change (increase versus decrease) varied at different locations along loop F. An increase in fluorescence for A5m indicates that the environment surrounding the attached fluorophore is increasing in hydrophobicity, whereas a decrease in fluorescence indicates a decrease in hydrophobicity. We interpret these changes in fluorescence as structural changes around the fluorophore. In a previous study using this approach, we considered the possibility that the change in fluorescence could result from quenching of the fluorophore by the ligand itself. The potential problem of quenching was previously refuted in this same system in other regions of the binding pocket (16). In the study presented here, this potential problem is even less likely because loop F is quite distant from the ligand molecule (Fig. 1).

Of the 14 residues analyzed, 11 showed a fluorescence change when GABA was applied. For three of the loop F residues (D219C, S225C, and L228C), however, there was no observed change in fluorescence in response to GABA application. This raises the question as to whether these positions were accessible by A5m. To address this issue, dose-response relations were measured before and after incubation in A5m. In the case of D219C and L228C, labeling with A5m imparted a significant change in the GABA sensitivity, suggesting that these positions are indeed accessible and labeled (Table 1). In contrast, the agonist sensitivity of S225C was the same before and after A5m exposure (Table 1). At this time, we are unable to confirm whether this is because the cysteine was not accessible to A5m, or there was labeling but no change in GABA sensitivity.

We will delay a detailed consideration of the implications of these ΔF values until the Discussion; however, a few features of these data are worth pointing out here. First, a majority of the positions demonstrate a ΔF, indicating that all of loop F is undergoing an environmental change. Second, there are some interesting features in the pattern of these changes. Note that there can be changes in fluorescence of opposite sign at adjacent residues (L216C, K217C, and T218C). This difference in ΔF at adjacent positions confirms that we are likely observing a structural rearrangement of (or around) loop F rather then a direct response (quenching) imparted by the presence of the GABA molecule itself. Also note that at the bend of loop F, namely S223C–F227C, the ΔF decreased, suggesting that upon activation the environment around this particular section becomes more exposed to the aqueous phase. Molecular-dynamics studies have also shown that this region in nACh receptors moves into a more aqueous environment upon activation (33).

Comparison of GABA-mediated changes in fluorescence and current in response to agonists, partial agonists, and competitive antagonists

If loop F were indeed a structural element coupling agonist binding to the opening of the pore, then, in its simplest form, this hypothesis would predict a correlation between the change in fluorescence and the degree of receptor activation. To test this hypothesis, we employed partial agonists and competitive antagonists. Partial agonists bind to the same site as that of GABA, but do not fully activate the receptor. Competitive antagonists are an extreme example of a partial agonist in that they also bind to the same site, but do not activate the receptor at all. This approach will enable us to examine receptors under conditions with comparable binding-site occupancy but exhibit a range of maximal receptor activations.

For this analysis we focused on the five positions in loop F that gave robust, consistent changes in current and fluorescence, and produced only modest shifts in sensitivity with cysteine mutagenesis and A5m labeling. These five positions are distributed throughout loop F, and we therefore assume that the fluorescence changes at these positions reflect structural rearrangements of (or around) this entire domain. Fig. 4 shows representative ΔF and ΔI values in response to GABA and/or TACA (full agonists), I4AA and/or isoguvacine (partial agonists), and 3-APA (competitive antagonist), all at saturating concentrations (excluding I4AA for L216C, as mentioned in Materials and Methods). We also show data for L166C, a residue in loop E of the binding site (Fig. 1 *A*), and this will be discussed subsequently. Bar graphs are provided that plot the ΔF and ΔI for each ligand normalized to that of GABA. First, note that comparison of the relative magnitudes of the agonist-mediated currents (*black bars*, normalized to GABA) varies for a given agonist on the different mutants. For example, the partial agonist isoguvacine yielded currents that were 18%, 35%, and 65% that of GABA for L216C, K217C, and T218C, respectively. For comparison, the wild-type efficacies were GABA, 1.0; I4AA, 0.03 $\pm$ 0.00; and isoguvacine, 0.46 $\pm$ 0.01 ($n = 5$). Thus, the substitutions can alter the efficacy profile, and this is not unexpected since loop F is a structural component of the binding pocket. Still, in all cases, GABA or TACA is the most potent agonist, 3-APA is a competitive antagonist, and the other ligands fall somewhere in between these two extremes in terms of activation and are therefore partial agonists.

A comparison of the I4AA data typifies the obvious lack of correlation between ΔF and ΔI. For L216C, K217C, T218C, and S223C, this partial agonist was of low efficacy, as revealed by the small current amplitudes, yet the ΔF was indistinguishable from that of GABA ($p < 0.05$). Another example of this lack of correlation is provided by 3-APA, the competitive antagonist. In all cases, no currents were elicited by 3-APA, although the ΔF values for L216C, K217C, and T218C were similar to that induced by the partial agonist isoguvacine. In the case of I229C, the ΔF for the competitive antagonist, 3-APA, was indistinguishable from that of the full agonist, GABA ($p > 0.05$). Although the normalized ΔF and ΔI values for the partial agonist isoguvacine were not quantitatively correlated to each other (e.g., constant ratio), they did show intermediate normalized values for all

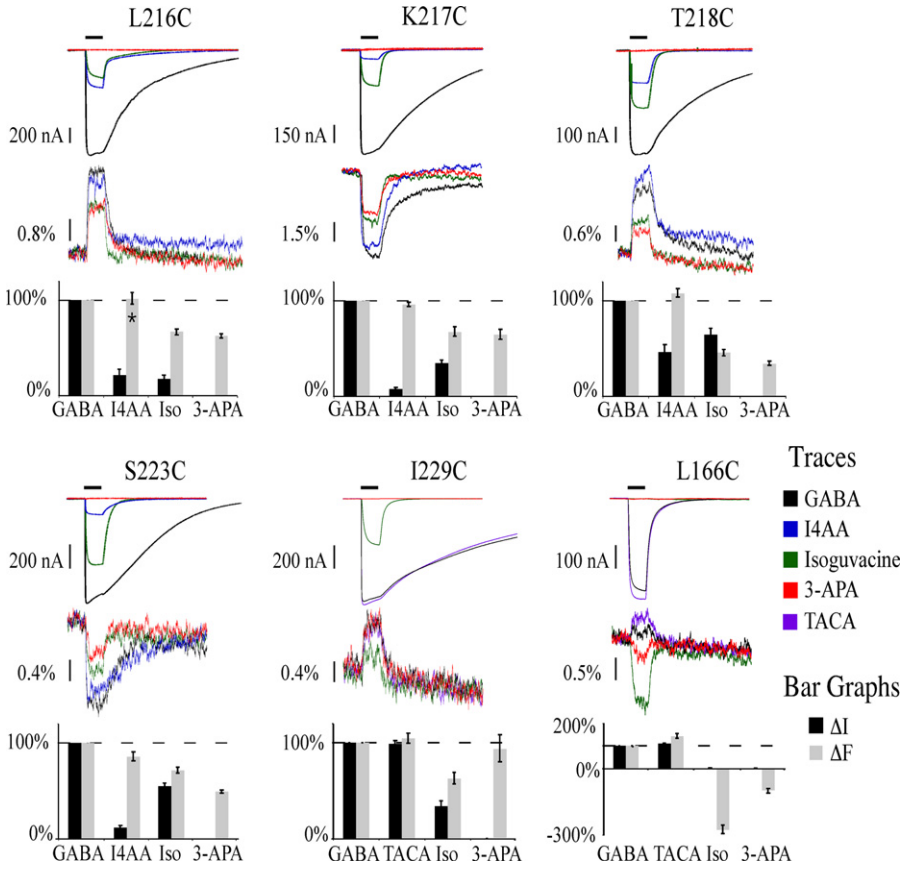

FIGURE 4 Correlation between current and fluorescence for a series of ligands. In all six panels, the top traces show the currents and the lower traces show the concomitant changes in fluorescence. GABA and TACA are full agonists, 3-APA is an antagonist, and I4AA and isoguvacine are partial agonists. Five loop F mutants, plus one mutation in loop E (L166C), are shown. The bar graphs plot the amplitude of the current (*solid*) and fluorescence (*gray*) normalized to that of GABA. *This was a subsaturating I4AA concentration, but note that the fluorescence is indistinguishable from that of a saturating concentration of the full agonist, GABA.

five loop F mutants. As described below, however, an examination of the entire array of mutants and ligands indicated that, as a whole, the ΔF and ΔI values were not correlated.

Fig. 5 is a scatter plot of the current versus fluorescence for each mutant and each agonist normalized to that for GABA. Each mutant is represented by a separate symbol, with the color indicating the particular agonist or antagonist. Although there is no a priori reason to assume a slope of one in this relation, if the ΔF observed in loop F upon activation represented the transduction between the binding of GABA and the opening of the pore (for example), some correlation would be evident. What is observed, however, is a clustering of the ΔF values based on the particular ligand but irrespective of the level of activation. It is worth noting from Fig. 5 that the competitive antagonist 3-APA spans the complete range of fluorescence changes, but in all cases generates no current. This is different from the ligands that open the channel and span a large range in their ΔI but a very limited range in their ΔF.

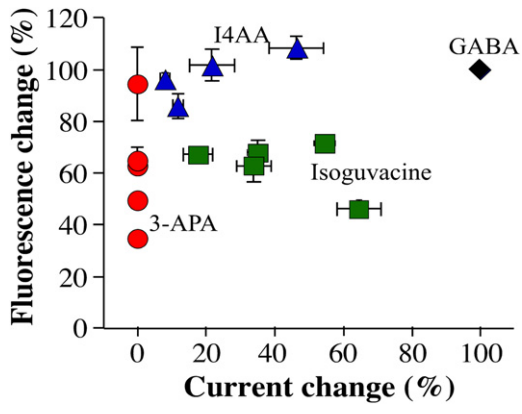

FIGURE 5 Relation between the change in current and change in fluorescence for the five loop F mutants. The amplitudes of the change in current and fluorescence were normalized to that of GABA and plotted against each other. The data seem to cluster by the particular agonist rather than the degree of activation.

To put these observations into perspective, data from the mutant L166C in loop E are shown in Fig. 4. Previous work on this mutation demonstrated fluorescence changes in response to GABA that are actually opposite in sign to that of the competitive antagonist (16). That earlier study concluded that structural rearrangements associated with this position reflect the degree of activation, at least for a full agonist (GABA) and a competitive antagonist (3-amino-propyl-(p-methyl)-phosphinic acid, or 3-APMPA). Fig. 4 (*lower right panel*) shows this correlation extended to other ligands. Whereas the full agonists GABA and TACA mediate comparable ΔF and ΔI values, 3-APA and isoguvacine produce no currents and have ΔF values opposite in sign to that of the full agonists. (In the case of the L166C mutation, isoguvacine has been converted from a partial agonist to an antagonist.) The observation that agonists

and antagonists produce ΔF values of opposite sign suggests that the structural rearrangements involving L166C are correlated with receptor activation.

Relation between the dose dependence of the current and ΔF

A previous study of the ρ1 GABA receptor demonstrated that radiolabeled agonist binding occurred at lower concentrations than receptor activation (34). Thus, ligand binding is detected at GABA concentrations where there is essentially no channel opening. This is a consequence of the activation mechanism of the ρ1 GABA receptor, where a minimum of three molecules of GABA are required to open the pore (7). If the structural rearrangements in loop F observed here are associated with GABA binding rather than receptor activation, we would predict that the dose dependence of ΔF, like that of ligand binding, occurs at lower agonist concentrations than channel opening. This approach of comparing the dose dependence of fluorescence and activation has also been employed in the nACh receptor at a position in the α-δ subunit interface to differentiate rearrangements associated with agonist binding versus latter steps in the activation process (35). The analysis requires the collection of ΔFs at low GABA concentrations, a difficult endeavor given the amplitude of our signals. We were successful, however, in constructing simultaneous and complete dose-response relations for ΔF and I in the K217C mutant. The results from these experiments are shown in Fig. 6. At this particular position, the dose dependence of ΔF occurred at lower GABA concentrations than the concomitant activation, with EC_{50} values of 0.90 ± 0.64 and 5.34 ± 1.25 ($n = 13$), respectively. These data are consistent with our hypothesis that the structural rearrangements in loop F signal ligand binding. Contrast this with data obtained in a previous study that looked at structural rearrangements at L166C, a position in loop E of the amino terminal domain (16). In that case, the dose dependence of ΔF and I were essentially superimposable, consistent with rearrangements of loop E being more closely correlated with receptor activation.

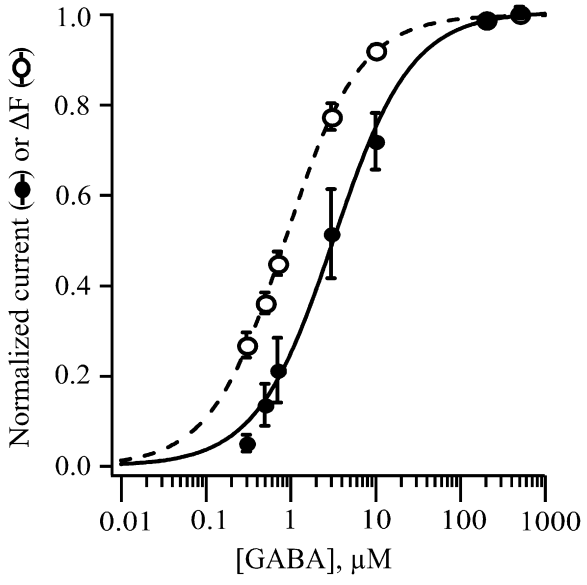

FIGURE 6 Dose dependence of current and ΔF at K217C. ΔF and I were measured simultaneously at a range of GABA concentrations. These data, normalized to their respective maxima, were then plotted as a function of GABA concentration. Note that ΔF occurred at GABA concentrations lower than that of channel opening. The Hill equation was fitted to these data, yielding EC_{50} values of 0.90 ± 0.64 and 5.34 ± 1.25, and Hill coefficients of 1.05 ± 0.085 and 1.56 ± 0.16 ($n = 13$) for ΔF and I, respectively.

DISCUSSION

The initial event in GABA receptor activation is the specific binding of agonist to its binding site located at subunit interfaces. Structure-function analyses, mainly employing site-directed mutagenesis, have identified the key residues that interact with ligand (8–15). These studies, along with the crystallization of AChBP, produced the six-loop model for the GABA-binding pocket considered in the Introduction (4). More recently, and in the study presented here, efforts have been made to elucidate the dynamics, or conformational rearrangements, that occur in the agonist-binding site in response to ligand binding, as well as the structures responsible for transducing this binding event to the gate, presumably formed by the transmembrane domains and near the center of the lipid bilayer (16–19). In this study, we focused our efforts on loop F, a candidate for a domain that couples ligand binding to channel opening in this cys loop family of receptors. Before proceeding with our working hypothesis, however, we should consider the assumptions and limitations of the experimental approach.

Assumptions and limitations

We employed a combination of electrophysiology and site-directed fluorescence spectroscopy to specifically address the role of loop F in activation of the homomeric ρ1 $GABA_C$ receptor. We made the working assumption that if structural rearrangements in loop F are crucial for triggering activation, these structural rearrangements should correlate with channel opening. We make the simplifying assumption that if two different ligands, when bound, produce similar changes in hydrophobicity, then the conformation of that region will likely be similar in the two cases. It is possible, however, that two very different and even opposite structural rearrangements could generate two similar fluorescence signals because the fluorophore moves into similar hydrophobic environments. We also reasoned that the conformation of the agonist-binding site would depend on the particular ligand bound. This reasoning was based on structural studies of glutamate receptors crystallized in the presence of agonists, partial agonists, and antagonists that concluded that the binding site adopts a conformation that correlates with

the degree of activation (36). Fluorescence spectroscopy studies on GABA receptors have also identified putative structural differences depending on whether agonists or antagonists are bound (16,18). In addition, studies in the glycine receptor using a similar approach as ours demonstrated distinct ΔF values in the external portion of the second transmembrane domain (M2) with the binding of agonists, partial agonists, and antagonists. Evidence indicates that this particular segment of the M2 domain may be important in the coupling between agonist binding and channel opening (37).

Finally, we have assumed that partial agonists produce a low maximum open probability compared to full agonists, owing to differences in the closed-to-open equilibrium (38). In this case, partial agonists stabilize the agonist-bound closed state relative to full agonists that tend to favor the agonist-bound open state. More recently, detailed single-channel analyses of the nACh and glycine receptors suggested that differences in the relative agonist efficacy occur at a state between agonist binding and channel opening (39). In either situation, the kinetic states visited by the receptor are the same for partial or full agonists, although the relative occupancies vary. In this case, if loop F were a transduction element undergoing a structural change upon activation, the observed steady-state fluorescence would represent the average fluorescence as the receptor flips back and forth between the activated and nonactivated positions (the simplest case). In this scenario, a correlation between the level of activation and the change in fluorescence would still be predicted since the steady-state fluorescence would be weighted by the relative occupancies of the two states.

Regarding limitations, our fluorescence approach does not allow us to derive the coordinates or magnitudes of structural movements, or even to determine whether loop F is moving (as opposed to the environment surrounding loop F). It does, however, report the degree of change in hydrophobicity surrounding the fluorophore. And lastly, the fluorescence being detected is at the fluorophore that is actually tethered to loop F through a roughly 15 Å linker.

The role of loop F

Several generalities regarding loop F were considered when we initiated this study. We will first consider the structural literature, followed by functional data. Structural resolution of the *Lymnaea stagnalis* AChBP loop F revealed a weakly resolved ''unusual'' conformation that is now considered a random coil (4). Structural resolution of the AChBP from *Aplysia californica* in complex with a series of agonists and antagonists indicates that loop F, along with loop C (Fig. 1 *A*), undergoes the largest rearrangement of any structure in the amino terminal domain (40). When compared with the unbound structure, and particularly relevant to our work, it appears that these conformational changes in loop F occur in response to agonists as well as antagonists (40). In terms of the refined 4 Å structure of the full-length *Torpedo marmorata*, there is little mention of loop F except to say that it does not extend down to the membrane-spanning domains (28). In contrast, hydrophobic photolabeling of the nACh receptor has indicated that loop F moves to a more hydrophobic environment, suggesting that this domain may make contact with the membrane surface (41).

Previous studies in which GABA was docked into the agonist-binding cleft of a structural model for the ρ1 $GABA_C$ receptor determined by homology with the *Lymnaea* AChBP revealed a series of possible orientations, all of which place loop F quite distant (5 Å) from the bound agonist molecule (42,43). Molecular-dynamics simulations in a structural model of the nACh receptor indicate a slight outward rotation of loop F and the removal of electrostatic contacts with the neighboring subunit during receptor activation (33). And finally, a recent dynamic analysis of the nACh receptor study concluded that loop F plays a role in local dynamics at the subunit interface and is likely involved in regulating binding affinity, but is probably not important in global channel motions (44).

Regarding functional information on the role of loop F in cys loop receptor activation, a SCAM analysis of loop F in the ρ1 $GABA_C$ receptor (10) demonstrated three points worth considering here. First, the cysteine mutations themselves (except for one position, Q226C) produced only very modest effects on receptor sensitivity. Second, nearly all the residues were accessible by the hydrophilic reagent [2-(trimethylammonium)ethyl]methanethiosulfonate bromide (MTSET) in both the open and the closed state. And third, the modifications by MTSET were not protected by the presence of agonist or antagonist. Taken together, these data suggest that residues in loop F probably do not interact with the bound ligand. Also, any structural changes imparted by the agonist do not bury the cysteine side chains in a hydrophobic, inaccessible environment. To summarize the structural and functional results, there is no definitive evidence that the rearrangements postulated to occur in loop F in response to agonist serve as a trigger for the conformational wave that leads to the opening of the pore.

When we examined five representative positions throughout loop F, with a series of agonists that went from full activation to complete antagonism, we observed no clear correlation between the magnitude of the current and fluorescence. Most notably, at four of the five positions, fluorescence changes were indistinguishable, although currents were either very small (I4AA, partial agonists) or absent (3-APA, antagonist). This led us to conclude that even though loop F may be rearranging in response to the presence of ligand, this domain is probably not along the transduction pathway leading to channel opening. Given this conclusion, it is interesting that some of the loop F cysteine mutations themselves altered the relative efficacy of the ligands. At face value, this observation seems to support a role of this domain in channel activation. However, the

inherent coupling between ligand binding and channel activation makes it a dangerous prospect to assign specific actions of a mutation on one versus the other (45,46). It is worth mentioning that a SCAM analysis of loop F in the related 5-HT_3 receptor also concluded that structural changes in this region depend on the presence of ligand, although not necessarily on whether the ligand is an agonist or antagonist (24).

Working hypothesis

GABA and 3-APA have comparable structures (Fig. 1 *C*), and 3-APA displays all the hallmarks of a classic competitive antagonist for GABA-mediated activation (47,48). It therefore stands to reason that the interactions between these ligands and the components of the binding pocket responsible for their affinities are similar. It is generally accepted that the structural rearrangements that occur upon agonist binding, in an ''induced-fit'' mechanism, close down around the ligand and trap it in the pocket. Our work on the ρ1 GABA receptor using the single oocyte binding technique has confirmed that channel opening locks GABA into the binding pocket (34). Although the interactions responsible for the affinities of GABA and 3-APA are likely similar, some key differences must certainly exist in the bound structures since GABA opens the pore but 3-APA does not. The structures of the full agonist, GABA, and the competitive antagonist, 3-APA, are identical at the amino end but very different at the carboxylic acid end, where 3-APA has a substituted phosphonic group (Fig. 1 *C*). If the orientation of GABA in the binding pocket is correct (Fig. 1 *A*), the amino group of the ligand (*blue*) would be positioned near loop C with the opposite end (oxygens indicated in *red*) pointed at loop E (*light blue*). This position and orientation agree with a previous study that placed the carboxylic acid group of GABA near arginine 158 on the E loop (43,49).

Loop C is a prominent protrusion in the binding pocket (Fig. 1 *A*) that extends across neighboring subunits (4). Upon agonist binding, loop C presumably closes the ligand-binding pocket by an inward movement (twist and rotation) toward its parent subunit (21,28,33,50–53). Loop C also contains residues that are crucial for ligand binding, including a well-conserved tyrosine that has been postulated (8,54) to play a direct role in stabilizing the agonist molecule, perhaps via π electrons associated with the aromatic ring (55,56). If the docked location of GABA depicted in Fig. 1 *A* is correct, then loop C may not distinguish agonist versus antagonist since it is proximate to the similar amino ends of the ligand. Note that loop F actually connects loops A and C, and loop A has also been postulated to be an important determinant for receptor affinity (10,13). Based on our data, and by virtue of the close association and mechanical link to loop C, we propose that loop F is part of the machinery that locks ligand into the binding site. In support of this, there are naturally occurring mutations in loop F of the nACh ε subunit that appear to alter the microscopic binding affinity for ACh (57). The rearrangement we observe about loop F may simply be because it is a pivot point, or hinge, between loops A and C. It is also worth mentioning that loop F connects loops A and C of the neighboring binding site (Fig. 1 *A*). Therefore, loop F could be in a position to transduce any allosteric coupling between adjacent binding sites (58). In support of this, loop F of the γ2 subunit seems to transduce allosteric modulation by benzodiazepines in $\alpha1\beta2\gamma2$ GABA receptors (59–61).

We have shown previously (16), and extended the analysis here, that structural rearrangements in loop E (L166C) seem to reflect the degree of activation or antagonism since very different fluorescence changes (opposite in sign) were observed between ligands that activate and ligands that antagonize the receptor. A similar relation was demonstrated in a study using site-directed fluorescence spectroscopy in $\alpha1\beta2$ $GABA_A$ receptors (18). Of interest, loop E is adjacent in sequence to the amino terminal cys-cys loop that has been proposed to interact with the linker between TM2 and TM3 via a salt bridge network, thereby leading to channel opening (23,62–68). More specifically, isomerization of a conserved proline in the TM2-TM3 loop from the *trans* to *cis* conformation may couple the amino terminal domain structural rearrangements to the rearrangement of TM2 that opens the pore (69). Based on all available evidence, we are turning our attention to loop E as a structure that may sense the presence of agonist and initiate the conformational wave toward the gate to open the ion channel.

We thank Dr. Brian E. Erkkila for helpful insights and for reading an earlier version of this manuscript. This work was funded by a grant from the National Institute of Neurological Disorders and Stroke (NS035291).

REFERENCES

1. Roberts, E. 2000. Adventures with GABA: fifty years on. *In* GABA in the Nervous System: The View at Fifty Years. D. L. Martin and R. W. Olsen, editors. Lippincott Williams & Wilkins, Philadelphia. 1–24.
2. Sieghart, W. 2006. Structure, pharmacology, and function of GABAA receptor subtypes. *Adv. Pharmacol.* 54:231–263.
3. Chang, Y., and D. Weiss. 2000. Functional domains of GABA receptors. *In* GABA in the Nervous System: The View at Fifty Years. D. L. Martin and R. W. Olsen, editors. Lippincott Williams & Wilkins, Philadelphia. 127–140.
4. Brejc, K., W. J. van Dijk, R. V. Klaassen, M. Schuurmans, J. van der Oost, et al. 2001. Crystal structure of an ACh-binding protein reveals the ligand-binding domain of nicotinic receptors. *Nature*. 411:269–276.
5. Chang, Y., R. Wang, S. Barot, and D. S. Weiss. 1996. Stoichiometry of a recombinant $GABA_A$ receptor. *J. Neurosci.* 16:5415–5424.
6. Tretter, V., N. Ehya, K. Fuchs, and W. Sieghart. 1997. Stoichiometry and assembly of a recombinant $GABA_A$ receptor subtype. *J. Neurosci.* 17:2728–2737.
7. Amin, J., and D. S. Weiss. 1996. Insights into the activation of ρ1 GABA receptors obtained by coexpression of wild type and activation-impaired subunits. *Proc. R. Soc. Lond. B. Biol. Sci.* 263:273–282.
8. Amin, J., and D. S. Weiss. 1993. $GABA_A$ receptor needs two homologous domains of the β-subunit for activation by GABA but not by pentobarbital. *Nature*. 366:565–569.
9. Torres, V. E., and D. S. Weiss. 2002. Identification of a tyrosine in the agonist binding site of the homomeric ρ1 GABA receptor that,

when mutated, produces spontaneous opening. *J. Biol. Chem.* 277: 43741–43748.

10. Sedelnikova, A., C. D. Smith, S. O. Zakharkin, D. Davis, D. S. Weiss, et al. 2005. Mapping the ρ1 GABA(C) receptor agonist binding pocket. Constructing a complete model. *J. Biol. Chem.* 280:1535–1542.
11. Sigel, E., R. Baur, S. Kellenberger, and P. Malherbe. 1992. Point mutations affecting antagonist affinity and agonist dependent gating of $GABA_A$ receptor channels. *EMBO J.* 11:2017–2023.
12. Boileau, A. J., A. R. Evers, A. F. Davis, and C. Czajkowski. 1999. Mapping the agonist binding site of the $GABA_A$ receptor: evidence for a β-strand. *J. Neurosci.* 19:4847–4854.
13. Boileau, A. J., J. G. Newell, and C. Czajkowski. 2002. GABA(A) receptor β2 Tyr97 and Leu99 line the GABA-binding site. Insights into mechanisms of agonist and antagonist actions. *J. Biol. Chem.* 277: 2931–2937.
14. Holden, J. H., and C. Czajkowski. 2002. Different residues in the GABA(A) receptor α1T60-α1K70 region mediate GABA and SR-95531 actions. *J. Biol. Chem.* 277:18785–18792.
15. Wagner, D. A., C. Czajkowski, and M. V. Jones. 2004. An arginine involved in GABA binding and unbinding but not gating of the GABA(A) receptor. *J. Neurosci.* 24:2733–2741.
16. Chang, Y., and D. S. Weiss. 2002. Site specific fluorescence reveals distinct structural changes with GABA receptor activation and antagonism. *Nat. Neurosci.* 5:1163–1168.
17. Wagner, D. A., and C. Czajkowski. 2001. Structure and dynamics of the GABA binding pocket: A narrowing cleft that constricts during activation. *J. Neurosci.* 21:67–74.
18. Muroi, Y., C. Czajkowski, and M. B. Jackson. 2006. Local and global ligand-induced changes in the structure of the GABA(A) receptor. *Biochemistry.* 45:7013–7022.
19. Kloda, J. H., and C. Czajkowski. 2007. Agonist-, antagonist-, and benzodiazepine-induced structural changes in the α1 Met113-Leu132 region of the $GABA_A$ receptor. *Mol. Pharmacol.* 71:483–493.
20. Chang, Y., and D. S. Weiss. 1998. Substitutions of the highly conserved M2 leucine create spontaneously opening ρ1 γ-aminobutyric acid receptors. *Mol. Pharmacol.* 53:511–523.
21. Unwin, N., A. Miyazawa, J. Li, and Y. Fujiyoshi. 2002. Activation of the nicotinic acetylcholine receptor involves a switch in conformation of the α subunits. *J. Mol. Biol.* 319:1165–1176.
22. Newell, J. G., and C. Czajkowski. 2003. The $GABA_A$ receptor α1 subunit Pro174-Asp191 segment is involved in GABA binding and channel gating. *J. Biol. Chem.* 278:13166–13172.
23. Kash, T. L., J. R. Trudell, and N. L. Harrison. 2004. Structural elements involved in activation of the γ-aminobutyric acid type A (GABAA) receptor. *Biochem. Soc. Trans.* 32:540–546.
24. Thompson, A. J., C. L. Padgett, and S. C. Lummis. 2006. Mutagenesis and molecular modeling reveal the importance of the $5\text{-}HT_3$ receptor F-loop. *J. Biol. Chem.* 281:16576–16582.
25. Karlin, A., and M. A. Akabas. 1998. Substituted cysteine accessibility method. *Methods Enzymol.* 293:123–145.
26. Wilson, G. G., and A. Karlin. 1998. The location of the gate in the acetylcholine receptor channel. *Neuron.* 20:1269–1281.
27. Miyazawa, A., Y. Fujiyoshi, M. Stowell, and N. Unwin. 1999. Nicotinic acetylcholine receptor at 4.6 A resolution: transverse tunnels in the channel wall. *J. Mol. Biol.* 288:765–786.
28. Unwin, N. 2005. Refined structure of the nicotinic acetylcholine receptor at 4A resolution. *J. Mol. Biol.* 346:967–989.
29. Dellisanti, C. D., Y. Yao, J. C. Stroud, Z. Z. Wang, and L. Chen. 2007. Crystal structure of the extracellular domain of nAChR α1 bound to α-bungarotoxin at 1.94 A resolution. *Nat. Neurosci.* 10:953–962.
30. Hilf, R. J., and R. Dutzler. 2008. X-ray structure of a prokaryotic pentameric ligand-gated ion channel. *Nature.* 452:375–379.
31. Mannuzzu, L. M., M. M. Moronne, and E. Y. Isacoff. 1996. Direct physical measure of conformational rearrangement underlying potassium channel gating. *Science.* 271:213–216.
32. Gandhi, C. S., E. Loots, and E. Y. Isacoff. 2000. Reconstructing voltage sensor-pore interaction from a fluorescence scan of a voltage-gated K^+ channel. *Neuron.* 27:585–595.
33. Cheng, X., H. Wang, B. Grant, S. M. Sine, and J. A. McCammon. 2006. Targeted molecular dynamics study of C-loop closure and channel gating in nicotinic receptors. *PLoS Comput. Biol.* 2:e134.
34. Chang, Y., and D. S. Weiss. 1999. Channel opening locks agonist onto the $GABA_C$ receptor. *Nat. Neurosci.* 2:219–225.
35. Dahan, D. S., M. I. Dibas, E. J. Petersson, V. C. Auyeung, B. Chanda, et al. 2004. A fluorophore attached to nicotinic acetylcholine receptorβ M2 detects productive binding of agonist to the α-δ site. *Proc. Natl. Acad. Sci. USA.* 101:10195–10200.
36. Jin, R., T. G. Banke, M. L. Mayer, S. F. Traynelis, and E. Gouaux. 2003. Structural basis for partial agonist action at ionotropic glutamate receptors. *Nat. Neurosci.* 6:803–810.
37. Pless, S. A., M. I. Dibas, H. A. Lester, and J. W. Lynch. 2007. Conformational variability of the glycine receptor M2 domain in response to activation by different agonists. *J. Biol. Chem.* 282:36057–36067.
38. Del Castillo, J., and B. Katz. 1957. Interaction at end-plate receptors between different choline derivatives. *Proc. R. Soc. Lond. B. Biol. Sci.* 146:369–381.
39. Lape, R., D. Colquhoun, and L. G. Sivilotti. 2008. On the nature of partial agonism in the nicotinic receptor superfamily. *Nature.* 454: 722–727.
40. Hansen, S. B., G. Sulzenbacher, T. Huxford, P. Marchot, P. Tayloret, et al. 2005. Structures ofAplysia AChBP complexes with nicotinic agonists and antagonists reveal distinctive binding interfaces and conformations. *EMBO J.* 24:3635–3646.
41. Leite, J. F., M. P. Blanton, M. Shahgholi, D. A. Dougherty, and H. A. Lester. 2003. Conformation-dependent hydrophobic photolabeling of the nicotinic receptor: electrophysiology-coordinated photochemistry and mass spectrometry. *Proc. Natl. Acad. Sci. USA.* 100:13054–13059.
42. Harrison, N. J., and S. C. Lummis. 2006. Molecular modeling of the GABA(C) receptor ligand-binding domain. *J. Mol. Model.* 12:317–324.
43. Abdel-Halim, H., J. R. Hanrahan, D. E. Hibbs, G. A. Johnston, and M. Chebib. 2008. A molecular basis for agonist and antagonist actions at GABA(C) receptors. *Chem. Biol. Drug Des.* 71:306–327.
44. Szarecka, A., Y. Xu, and P. Tang. 2007. Dynamics of heteropentameric nicotinic acetylcholine receptor: implications of the gating mechanism. *Proteins.* 68:948–960.
45. Colquhoun, D. 1998. Binding, gating, affinity and efficacy: the interpretation of structure-activity relationships for agonists and of the effects of mutating receptors. *Br. J. Pharmacol.* 125:923–947.
46. Colquhoun, D., and M. Farrant. 1993. The binding issue. *Nature.* 366:510–511.
47. Vien, J., R. K. Duke, K. N. Mewett, G. A. Johnston, R. Shingai, et al. 2002. trans-4-Amino-2-methylbut-2-enoic acid (2-MeTACA) and (+/−)-trans-2-aminomethylcyclopropanecarboxylic acid ((+/−)-TAMP) can differentiate rat ρ3 from human ρ1 and ρ2 recombinant GABA(C) receptors. *Br. J. Pharmacol.* 135:883–890.
48. Woodward, R. M., L. Polenzani, and R. Miledi. 1993. Characterization of bicuculline/baclofen-insensitive (ρ-like) γ-aminobutyric acid receptors expressed in *Xenopus* oocytes. II. Pharmacology of γ-aminobutyric $acid_A$ and γ-aminobutyric $acid_B$ receptor agonists and antagonists. *Mol. Pharmacol.* 43:609–625.
49. Harrison, N. J., and S. C. Lummis. 2006. Locating the carboxylate group of GABA in the homomeric rho GABA(A) receptor ligand-binding pocket. *J. Biol. Chem.* 281:24455–24461.
50. Gao, F., N. Bren, T. P. Burghardt, S. Hansen, R. H. Henchman, et al. 2005. Agonist-mediated conformational changes in acetylcholine-binding protein revealed by simulation and intrinsic tryptophan fluorescence. *J. Biol. Chem.* 280:8443–8451.
51. Law, R. J., R. H. Henchman, and J. A. McCammon. 2005. A gating mechanism proposed from a simulation of a human α7 nicotinic acetylcholine receptor. *Proc. Natl. Acad. Sci. USA.* 102:6813–6818.

52. Celie, P. H., S. E. van Rossum-Fikkert, W. J. van Dijk, K. Brejc, A. B. Smit, et al. 2004. Nicotine and carbamylcholine binding to nicotinic acetylcholine receptors as studied in AChBP crystal structures. *Neuron.* 41:907–914.

53. Lee, W. Y., and S. M. Sine. 2005. Principal pathway coupling agonist binding to channel gating in nicotinic receptors. *Nature.* 438: 243–247.

54. Amin, J., and D. S. Weiss. 1994. Homomeric ρ1 GABA channels: activation properties and domains. *Receptors Channels.* 2:227–236.

55. Lummis, S. C., L. D. Beene, N. J. Harrison, H. A. Lester, and D. A. Dougherty. 2005. A cation-π binding interaction with a tyrosine in the binding site of the $GABA_C$ receptor. *Chem. Biol.* 12:993–997.

56. Padgett, C. L., A. P. Hanek, H. A. Lester, D. A. Dougherty, and S. C. Lummis. 2007. Unnatural amino acid mutagenesis of the GABA(A) receptor binding site residues reveals a novel cation-π interaction between GABA and β 2Tyr97. *J. Neurosci.* 27:886–892.

57. Sine, S. M., X. M. Shen, H. L. Wang, K. Ohno, W. Y. Lee, et al. 2002. Naturally occurring mutations at the acetylcholine receptor binding site independently alter ACh binding and channel gating. *J. Gen. Physiol.* 120:483–496.

58. Changeux, J. -P., and S. J. Edelstein. 1998. Allosteric receptors after 30 years. *Neuron.* 21:959–980.

59. Hanson, S. M., and C. Czajkowski. 2008. Structural mechanisms underlying benzodiazepine modulation of the $GABA_A$ receptor. *J. Neurosci.* 28:3490–3499.

60. Padgett, C. L., and S. C. Lummis. 2008. The F-loop of the GABA A receptor γ2 subunit contributes to benzodiazepine modulation. *J. Biol. Chem.* 283:2702–2708.

61. Sancar, F., S. S. Ericksen, A. M. Kucken, J. A. Teissere, and C. Czajkowski. 2007. Structural determinants for high-affinity zolpidem binding to GABA-A receptors. *Mol. Pharmacol.* 71:38–46.

62. Kash, T. L., M. J. Dizon, J. R. Trudell, and N. L. Harrison. 2004. Charged residues in the β2 subunit involved in $GABA_A$ receptor activation. *J. Biol. Chem.* 279:4887–4893.

63. Kash, T. L., A. Jenkins, J. C. Kelley, J. R. Trudell, and N. L. Harrison. 2003. Coupling of agonist binding to channel gating in the GABA(A) receptor. *Nature.* 421:272–275.

64. Kash, T. L., T. Kim, J. R. Trudell, and N. L. Harrison. 2004. Evaluation of a proposed mechanism of ligand-gated ion channel activation in the $GABA_A$ and glycine receptors. *Neurosci. Lett.* 371:230–234.

65. Absalom, N. L., T. M. Lewis, W. Kaplan, K. D. Pierce, and P. R. Schofield. 2003. Role of charged residues in coupling ligand binding and channel activation in the extracellular domain of the glycine receptor. *J. Biol. Chem.* 278:50151–50157.

66. Lyford, L. K., A. D. Sproul, D. Eddins, J. T. McLaughlin, and R. L. Rosenberg. 2003. Agonist-induced conformational changes in the extracellular domain of α7 nicotinic acetylcholine receptors. *Mol. Pharmacol.* 64:650–658.

67. Sala, F., J. Mulet, S. Sala, S. Gerber, and M. Criado. 2005. Charged amino acids of the N-terminal domain are involved in coupling binding and gating in α7 nicotinic receptors. *J. Biol. Chem.* 280:6642–6647.

68. Xiu, X., A. P. Hanek, J. Wang, H. A. Lester, and D. A. Dougherty. 2005. A unified view of the role of electrostatic interactions in modulating the gating of Cys loop receptors. *J. Biol. Chem.* 280:41655–41666.

69. Lummis, S. C., D. L. Beene, L. W. Lee, H. A. Lester, R. W. Broadhurst, et al. 2005. *Cis-trans* isomerization at a proline opens the pore of a neurotransmitter-gated ion channel. *Nature.* 438:248–252.